Neuropharmacology 88 (2015) 82–90

Contents lists available at ScienceDirect

Neuropharmacology

journal homepage: www.elsevier.com/locate/neuropharm

Activation of calcineurin underlies altered trafficking of α2 subunit containing $GABA_A$ receptors during prolonged epileptiform activity

Ramona Eckel [a, b], Blanka Szulc [b], Matthew C. Walker [a, *], Josef T. Kittler [b, *]

[a] Department of Clinical and Experimental Epilepsy, Institute of Neurology, University College London, London, UK
[b] Department of Neuroscience, Physiology and Pharmacology, University College London, London, UK

ARTICLE INFO

Article history:
Available online 22 September 2014

Keywords:
$GABA_A$ receptor
Trafficking
Surface stability
Epilepsy
Calcium signaling

ABSTRACT

Fast inhibitory signalling in the mammalian brain is mediated by gamma-aminobutyric acid type A receptors ($GABA_A$Rs), which are targets for anti-epileptic therapy such as benzodiazepines. $GABA_A$Rs undergo tightly regulated trafficking processes that are essential for maintenance and physiological modulation of inhibitory strength. The trafficking of $GABA_A$Rs to and from the membrane is altered during prolonged seizures such as in Status Epilepticus (SE) and has been suggested to contribute to benzodiazepine pharmacoresistance in patients with SE. However, the intracellular signalling mechanisms that cause this modification in $GABA_A$R trafficking remain poorly understood. In this study, we investigate the surface stability of $GABA_A$Rs during SE utilising the low Mg^{2+} model in hippocampal rat neurons. Live-cell imaging of super ecliptic pHluorin (SEP)-tagged α_2 subunit containing $GABA_A$Rs during low Mg^{2+} conditions reveals that the somatic surface receptor pool undergoes down-regulation dependent on N-methyl-D-aspartate receptor (NMDAR) activity. Analysis of the intracellular Ca^{2+} signal during low Mg^{2+} using the Ca^{2+}-indicator Fluo4 shows that this reduction of surface $GABA_A$Rs correlates well with the timeline of intracellular Ca^{2+} changes. Furthermore, we show that the activation of the phosphatase calcineurin was required for the decrease in surface $GABA_A$Rs in neurons undergoing epileptiform activity. These results indicate that somatic modulation of $GABA_A$R trafficking during epileptiform activity *in vitro* is mediated by calcineurin activation which is linked to changes in intracellular Ca^{2+} concentrations. These mechanisms could account for benzodiazepine pharmacoresistance and the maintenance of recurrent seizure activity, and reveal potential novel targets for the treatment of SE.

This article is part of the Special Issue entitled 'GABAergic Signaling in Health and Disease'.

1. Introduction

$GABA_A$ Receptors ($GABA_A$Rs) are ligand-gated chloride permeable ion channels which mediate both phasic (synaptic) and tonic (extrasynaptic) inhibitory neurotransmission in the central nervous system (Jacob et al., 2008; Luscher et al., 2011). They assemble from five subunits, the composition of which determines the receptors functional and pharmacological properties and the specific location on the neuronal membrane (Luscher et al., 2011; Jacob et al., 2008). $GABA_A$Rs containing the γ2 subunit mediate synaptic transmission (in contrast to extrasynaptic receptors located away from the synapse) and are a target for benzodiazepines (Pritchett et al., 1989).

The enrichment of $GABA_A$Rs in subcellular compartments such as the axon initial segment (AIS) has been reported for the α2 subunit and although both α1 and α2 subunits are found at the synapse in dendrites, a minority of $GABA_A$Rs in the AIS contain the α1 subunit (Panzanelli et al., 2011; Brünig et al., 2002). $GABA_A$Rs undergo dynamic movement within the cellular membrane. Lateral diffusion facilitates trafficking and assures the appropriate surface localisation of the receptor (Mukherjee et al., 2011), while trafficking to and from the membrane through exocytotic and endocytotic processes allows constant maintenance of the inhibitory synaptic receptor pool (Bogdanov et al., 2006; Kittler et al., 2000, 2004). Altered neuronal activity causes surface $GABA_A$Rs to undergo plasticity-induced trafficking changes. These are mediated by alterations in the activity of protein phosphatases and kinases which are linked to changes in intracellular Ca^{2+} (Muir et al., 2010; Bannai et al., 2009; Saliba et al., 2012; Luscher et al., 2011; Jacob et al., 2008; Petrini et al., 2014).

* Corresponding authors.
E-mail addresses: m.walker@ucl.ac.uk (M.C. Walker), j.kittler@ucl.ac.uk (J.T. Kittler).

http://dx.doi.org/10.1016/j.neuropharm.2014.09.014

SE evolves rapidly and dynamically, manifesting as a prolonged and self-sustaining seizure with significant morbidity and mortality (Lothman, 1990; Dodrill and Wilensky, 1990; Sutter et al., 2013). This distinct condition can occur in patients with previous epilepsy or may occur *de novo* as a result of acute neurological disorders (Trinka et al., 2012). As SE evolves, the patient's response to treatment with benzodiazepines decreases progressively which rapidly results in benzodiazepine pharmacoresistance. This may lead to refractory SE, a pathological state in which seizures are not sopped by first- or second-line anticonvulsant therapies.

To unravel the role of benzodiazepine pharmacoresistance associated with SE patients, studies have addressed whether the trafficking of $GABA_A$Rs to and from the cellular membrane is altered during models of SE (Naylor et al., 2005; Goodkin et al., 2005; Blair et al., 2004). Interestingly, it has been suggested that $GABA_A$Rs are subjected to subunit-specific trafficking during prolonged depolarisation. $GABA_A$Rs containing the synaptic subunits β2/3 and γ2 undergo internalisation whereas those containing the extrasynaptic δ subunit remain unchanged (Goodkin et al., 2008). Despite recent studies, the temporal dynamics of $GABA_A$R trafficking have not been investigated using live-cell imaging. Moreover, whether endocytosis occurs preferentially in distinct compartments such as dendrites or soma remains unclear. It is not known which molecular pathways underlie this subunit-specific trafficking of $GABA_A$Rs. Furthermore, it remains to be determined whether Ca^{2+} and its intracellular signalling cascades play a significant role in the modulation of GABAergic inhibition during SE.

To address the molecular mechanisms underlying altered $GABA_A$R trafficking during SE, we used a live-cell imaging approach to examine the surface stability of $GABA_A$Rs in hippocampal neurons. We induced prolonged epileptiform bursting activity *in vitro* by exposing neurons to artificial cerebrospinal fluid (aCSF) lacking Mg^{2+} (Mangan and Kapur, 2004; Sombati and Delorenzo, 1995). Using this model, we show a decrease in somatic surface $GABA_A$Rs that is dependent on NMDAR activity and the Ca^{2+}-dependent phosphatase, calcineurin. Furthermore, we show that epileptiform activity alters intracellular Ca^{2+} concentrations, which correlates with the decrease of $GABA_A$Rs from the surface possibly contributing to pathological signalling during SE.

2. Materials and methods

2.1. Constructs

The N-terminally tagged $GABA_A$ α_2-$_{SEP}$ DNA was a kind gift from S. Moss (Tufts University, Cambridge, MA) and has been described previously (Tretter et al., 2008).

2.2. Cell culture and transfection

All animal experiments were carried out in accordance with the U.K. Animals (Scientific Procedures) Act, 1986. All efforts were made to minimise animal suffering and to reduce the number of animals used. Dissected hippocampi of P0 rat pups or E18 embryos were immediately placed in ice-cold dissection buffer (HBSS (Invitrogen)) and washed once. Using trypsin (0.25%) tissue was digested for 10 min before trituration in ~2 ml of attachment medium. Neurons were plated onto poly-L-lysine (Sigma) coated coverslips (500 μg/ml). For nucleofection, hippocampal neurons were nucleofected with $GABA_A$ α_{2SEP} plasmid DNA. Neurons were centrifuged and the cell pellet was resuspended in 100 μl transfection buffer (135 mM KCL, 10 mM HEPES-pH 7.3, 2 mM $MgCl_2$, 5 mM EGTA, 0.2 mM $CaCl_2$) and transfected using a single cuvette AMAXA system (Lonza, programme O-003 or AK-009). Neurons were left to develop at 37 °C and 95% O_2, 5% CO_2 in maintenance medium [Neurobasal (Invitrogen), B27 Supplement (Invitrogen), 0.6% Glucose (Sigma), 2 mM Glutamine (Invitrogen) and Penicillin–Streptomycin] for 14–21 DIV before imaging.

2.3. Live-cell imaging

Live-cell imaging was performed on an upright Olympus microscope (BX51WI) coupled to an EM-CCD camera (Ixon, Andor). Cells were imaged with a water-immersion 60× objective (Olympus). Excitation was provided by an X-cite 120Q light source (Lumen Dynamics). Appropriate filters were used (in nm): Excitation: 470/40; Emission: 525/50; Dichroic: 495, long pass. The image pixel scale was calculated by dividing the camera pixel size (16 μm) by the lens magnification (60×) yielding a pixel size of 0.27 μm. Before constant perfusion with a Cole–Parmer Master-Flex pump (~4 ml/min), aCSF (126 mM NaCl, 24 mM $NaHCO_3$, 10 mM D-Glucose, 2.5 mM KCL, 2 mM $CaCl_2$, 1 mM MgCl, 1 mM NaH_2PO_4, 5 mM Sodium Pyruvate) was pre-equilibrated for 20 min with 95% O_2 and 5% CO_2 to establish a pH of 7.4. Temperature of the waterbath was constantly measured using a digital Thermometer (Hanna Instruments) and maintained at 37 °C. Any focus drift was corrected manually. Protocols were adapted to achieve minimal bleaching conditions. Imaging of SEP-tagged $GABA_A$Rs was done for 60 min at a rate of one frame every 20 s (180 frames, 48.8 ms exposure, no averaging). For imaging of intracellular Ca^{2+} using fluo4 (1 μM, Molecular Probes, Invitrogen) hippocampal neurons were incubated for 30 min at 37 °C. After washing twice, fluo4-imaging was done for 60 min (720 frames, 5 ms exposure, no averaging) at 1 frame every 5 s.

2.4. Cell-attached recording

Cell-attached recordings were made on transfected hippocampal neurons at 13 DIV using an Axopatch 200B amplifier (Molecular Devices) and pClamp software. Cells were visualised using an upright Olympus BX50WI microscope equipped with a 40× water-immersion objective and infrared optics. Recording electrodes were pulled from standard-walled borosilicate glass capillaries (Warner Instruments) and filled with aCSF. Gigaseal cell attached recordings were made in voltage-clamp mode at −70 mV; the cells were constantly perfused with aCSF. To block currents during recording NBQX disodium salt (20 μM, Abcam) and dAPV (D-(−)-2-Amino-5-phosphonopentanoic acid, 25 μM, TOCRIS) were added to the perfusion solution.

2.5. Low Mg^{2+} and drug treatments

To induce epileptiform bursting activity, aCSF without Mg^{2+} but 2 μM glycine (126 mM NaCl, 24 mM $NaHCO_3$, 10 mM D-Glucose, 2.5 mM KCL, 2 mM $CaCl_2$, 1 mM NaH_2PO_4, 5 mM sodium pyruvate, 2 μM glycine) was used (Blair et al., 2004). We confirmed previous studies (Robinson et al., 1993; Mangan and Kapur, 2004; DeLorenzo et al., 1998) that low Mg^{2+} results in cellular burst spiking that is dependent upon glutamateric transmission (Sup. Fig.2). Moreover, action potentials were associated with post-synaptic currents, indicating that the bursting was the result of network activity (Sup. Fig. 2). The mitochondrial substrate sodium pyruvate was supplemented to reduce neuronal death (Kovac et al., 2012). Transfected hippocampal neurons were perfused with control aCSF for 3.3 min (10 frames, baseline), followed by either low Mg^{2+} treatment or continued perfusion with aCSF with Mg^{2+} (control) for 60 min. To block NMDAR activity during low Mg^{2+} treatment, the NMDAR blocker dAPV (25 μM, TOCRIS) was used continuously throughout the low Mg^{2+} treatment without preincubation. For low Mg^{2+}/NMDA treatment, NMDA (30 μM, TOCRIS) was added to the low Mg^{2+} medium and applied continuously for 60 min. To block the activity of the Ca^{2+} dependent phosphatase calcineurin, cells were pre-incubated with calcineurin autoinhibitory peptide (Terada et al., 2003) (50 μM, Calbiochem) for 25 min at 37 °C and imaged (without application of the peptide during perfusion) either during control or low Mg^{2+} treatment (Muir et al., 2010).

2.6. Image analysis

Intensity analysis of specific regions of interests (ROIs: background, soma, diffuse, clustered) was done in ImageJ 1.43u which allowed the export of raw data to MatlabR2008a Software. Image correction was done in ImageJ software using the plugin StackReg macro (Thévenaz et al., 1998) which corrects for drift in (*x*,*y*). Inverted average intensity projection was done in ImageJ by using the Z-stack application from frame 1–10 (0–3 min) and frame 30–60 (10–20 min). Analysis of SEP-imaging raw data was done using Matlab Software through a custom designed code. Background was subtracted from each frame, fluorescence intensity was normalised to the baseline (average value of $t = 0$–3.33 min) and averaged for each experimental group. The fluorescence intensity values for each specific ROI were analysed in individual loops which allowed separate analysis. Furthermore, the standard error of mean (SEM) was calculated for each time-point and the mean normalised values including error bars were plotted against time. Ca^{2+} imaging was analysed using ImageJ. Fluorescence intensity in the soma was extracted from one ROI per cell. Baseline for 60 min Ca^{2+}-imaging was the average of the first 10 frames ($t = 0$–50 s), which corresponds to control conditions.

2.7. Statistical analysis

All experiments were performed on neurons from at least three individual preparations. The software GraphPad Prism was used for statistical tests and to generate bar charts. Data sets were tested to determine if they were normally distributed (KS normality test) before undertaking further statistical analysis. For low Mg^{2+} only and low Mg^{2+} NMDA treatments, *p* values were determined using a Student's *t* test (two-tailed). Repeat measures ANOVA (for normally distributed data) or Friedman test was used to analyse significance of low Mg^{2+} induced effects during Ca^{2+}-imaging, low Mg^{2+}/dAPV and low Mg^{2+}/CAIP experiments since there were more than two experimental groups. Appropriate post-hoc tests such as Tukey's for normally distributed data or Dunn's multiple comparison for non-normally distributed data were used. Values are given as mean ± SEM. Error bars represent SEM.

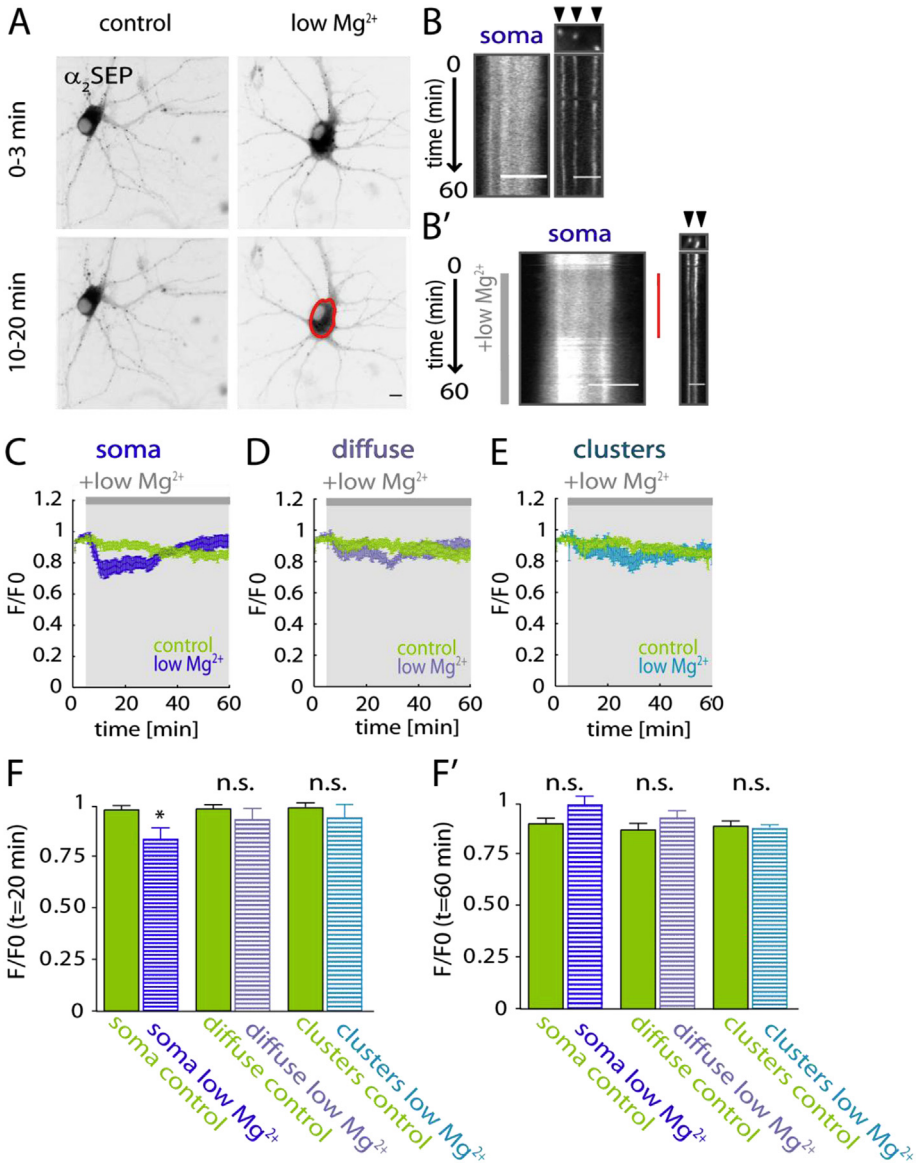

Fig. 1. Somatic surface α_{2SEP}-GABA$_A$Rs decrease upon low Mg^{2+} treatment. (A) Representative average intensity projection of α_{2SEP} expression in control and low Mg^{2+} treated neurons over time (0–3 min and 10–20 min). Scale bar, 10 μm. (B) Kymograph (a line scan vertically projected over time) showing somatic (left; scale bar, 5 μm) and clustered (right; arrow heads indicate clusters; scale bar, 2 μm) α_{2SEP} fluorescence intensity over the movie in control (aCSF) conditions and in the presence of low Mg^{2+} (grey bar). Red bar on the right indicates a decrease in somatic fluorescence intensity upon low Mg^{2+} treatment. (C) Average fluorescence intensity of somatic α_{2SEP} GABA$_A$R F/F_0: control (green, $n = 9$ cells) and low Mg^{2+} (blue, $n = 7$). (D) Time course of diffuse α_{2SEP} GABA$_A$R F/F_0: control (green, $n = 9$ cells); low Mg^{2+} (purple, $n = 7$). (E) Time course of α_{2SEP} GABA$_A$R clusters F/F_0: control (green, $n = 9$ cells) and low Mg^{2+} (light blue, $n = 7$). (F) Bar graph of ROI's F/F_0: soma (left), diffuse (middle) clusters (right). Significant loss of fluorescence in the soma compared to control at 20 min following low Mg^{2+} treatment ($p = 0.02$). Diffuse fluorescence is not altered at 20 min ($p = 0.36$) after low Mg^{2+} treatment. Fluorescence intensity of α_{2SEP} GABA$_A$R clusters is unaltered following low Mg^{2+} treatment ($t = 20$ min; p = 0.28) compared to control. (F') At 60 min after low Mg^{2+} treatment somatic ($p = 0.09$), diffuse ($p = 0.85$) and clustered ($p = 0.42$) fluorescence intensity are not significantly altered.*$p < 0.05$. (For interpretation of the references to colour in this figure legend, the reader is referred to the web version of this article.)

3. Results

3.1. Surface stability of somatic GABA$_A$Rs in hippocampal neurons is altered during Low Mg^{2+} treatment

To examine the influence of SE on GABA$_A$R stability and clustering *in vitro*, we mimicked the characteristic repetitive epileptiform bursting activity of SE by removal of Mg^{2+} from the extracellular medium of cultured hippocampal rat neurons transfected with SEP-tagged GABA$_A$R α_2 subunit (α_{2SEP}) (Sombati and Delorenzo, 1995). Surface GABA$_A$Rs were imaged via the SEP-tag on the α_2 subunit (Muir et al., 2010) (which allows visualisation through high fluorescence in neutral pH, Sup. Fig.1) for 60 min. α_{2SEP} fluorescence was analysed in 3 distinct regions of interests (ROIs): soma, diffuse (extrasynaptic compartment in dendrites) and clusters. At t = 20 min, somatic fluorescence of α_{2SEP}-containing GABA$_A$Rs was significantly decreased (control F/F_0: 0.997 ± 0.02, low Mg^{2+} F/F_0: 0.85 ± 0.05; $p = 0.02$) indicating that internalisation of GABA$_A$Rs at the somatic level increases during low Mg^{2+} treatment (Fig. 1C,F). This could account for a decrease in hippocampal GABAergic inhibition during epileptiform activity. However, α_{2SEP}-fluorescence intensity at the soma was not found to be significantly changed at $t = 60$ min (control F/F_0: 0.92 ± 0.03, low Mg^{2+} F/F_0: 1.01 ± 0.04; $p = 0.09$) suggesting a biphasic regulation of surface

$GABA_AR$s during low Mg^{2+} treatment (Fig. 1C,F'). Interestingly, α_{2SEP}-$GABA_AR$ clusters (t = 20 min; control F/F_0: 1.02 ± 0.02 low Mg^{2+} F/F_0: 0.96 ± 0.07; p = 0.36) and diffuse (t = 20 min; control F/F_0: 1.01 ± 0.02, low Mg^{2+} F/F_0: 0.95 ± 0.05; p = 0.28) fluorescence intensity in the neuronal dendrites during low Mg^{2+} treatment showed only a minor, non-significant decrease. Our data thus indicates compartmental specificity of low Mg^{2+} induced decrease of $GABA_AR$s from the surface (Fig. 1D,E), with $GABA_AR$s primarily endocytosed from the cell soma surface.

3.2. Activity of NMDA receptors induces the down-regulation of somatic $GABA_A$ receptors from the surface during Low Mg^{2+} treatment

Low extracellular Mg^{2+} induces epileptiform activity which is abolished by application of the NMDAR antagonist dAPV (Coan and Collingridge, 1985, 1987; Tancredi et al., 1990; Albowitz et al., 1997; Westerhoff et al., 1995; Gulyás-Kovács et al., 2002; Mangan and Kapur, 2004). Therefore, we tested whether inhibition of NMDAR activity during low Mg^{2+} treatment blocks the somatic down-regulation of $GABA_AR$s (Fig. 2). Low Mg^{2+} alone induced a significant decrease of α_{2SEP}-$GABA_AR$ fluorescence intensity at t = 20 min whereas this loss was inhibited by the co-application of dAPV (t = 20 min; control F/F_0: 0.97 ± 0.05, low Mg^{2+} F/F_0: 0.65 ± 0.03 ($p < 0.001$), low Mg^{2+}/dAPV F/F_0: 0.96 ± 0.07 ($p > 0.05$); one-way ANOVA test, Tukey's multiple comparison post test), confirming that the down regulation of surface $GABA_AR$s was dependent on the activation of NMDARs (Fig. 2C,C').

3.3. Epileptiform activity evokes intracellular Ca^{2+} changes that correspond to the temporal dynamics of somatic surface $GABA_AR$ decrease

To further explore the mechanisms of NMDAR-driven decrease in surface $GABA_AR$s during low Mg^{2+} treatment, we applied the fluorescent Ca^{2+} indicator fluo4 in low Mg^{2+} treated hippocampal neurons. This allowed us to investigate intracellular Ca^{2+} transients evoked by low Mg^{2+} treatment. Hippocampal neurons perfused with control aCSF exhibit small Ca^{2+} transients reflecting spontaneous activity, whereas low Mg^{2+} perfusion significantly altered intracellular Ca^{2+} throughout the timeline of 60 min (Fig. 3B,B'). Fluo4 imaging reported intracellular Ca^{2+} increases rapidly upon early perfusion with low Mg^{2+} (10–20 min F/F_0: 375.8 ± 28.4; $p < 0.001$, Friedman test and Dunn's multiple comparison post test) and at t = 60 min (F/F_0: 215.2 ± 28.8; $p < 0.05$, Friedman test and Dunn's multiple comparison post test) in comparison to baseline (t = 100–150 s; F/F_0: 104.5 ± 4.4), (Fig. 3C). This indicates that low Mg^{2+} treatment induces an intracellular Ca^{2+} rise, which is likely to be caused by activation of NMDARs. Interestingly, intracellular Ca^{2+} concentration drops significantly during the timeline (10–20 min, F/F_0: 375.8 ± 28.4; 50–60 min, F/F_0: 215.2 ± 28.8; $p < 0.05$, Friedman test and Dunn's multiple comparison post test) showing that intracellular Ca^{2+} concentration undergoes alteration on a similar timescale to that of somatic surface $GABA_AR$ decrease (Fig. 3C).

3.4. Dispersion of clustered $GABA_A$ receptors is induced by NMDA receptor activation

It has been reported that the dispersal of surface $GABA_AR$ clusters in neuronal processes is regulated through Ca^{2+} influx via NMDARs (Muir et al., 2010). Therefore we tested whether further increasing the activation of NMDARs by co-application of low Mg^{2+} and the agonist NMDA would trigger dispersion of surface $GABA_AR$ clusters in proximal dendrites. Indeed, the activation of NMDARs with low Mg^{2+} in addition to application of the agonist NMDA (low

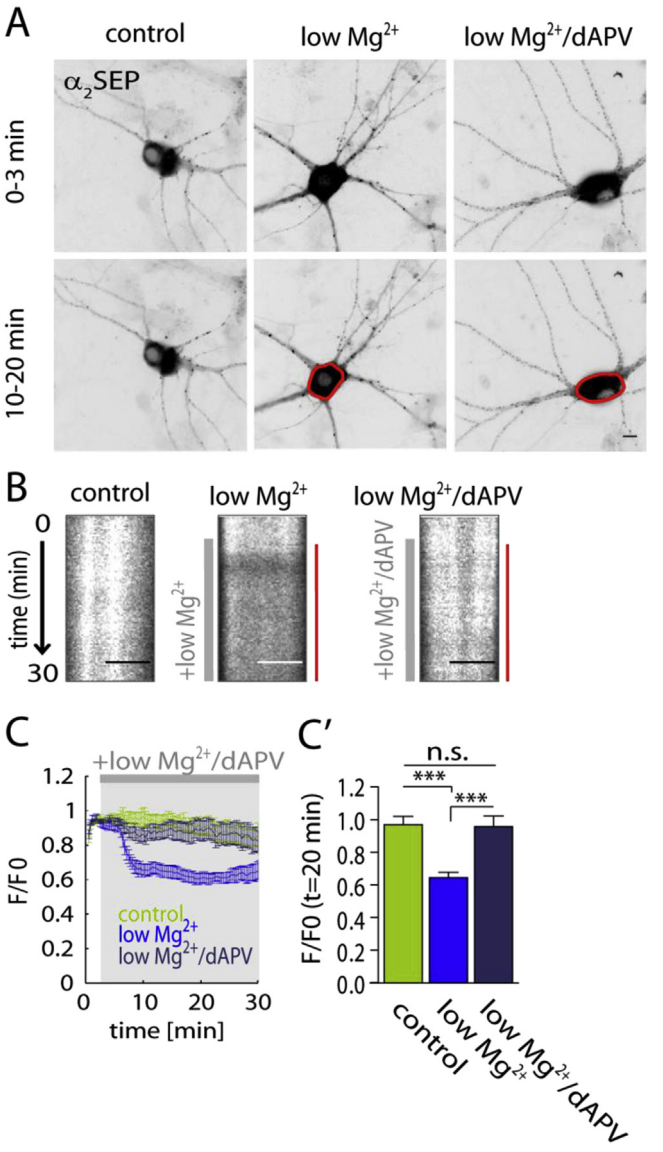

Fig. 2. NMDARs mediate low Mg^{2+} induced somatic α_{2SEP} $GABA_AR$ surface decrease. (A) Representative images of α_{2SEP} $GABA_AR$ fluorescence in control, low Mg^{2+} and low Mg^{2+} with dAPV (low Mg^{2+}/dAPV) treated neurons as an average intensity projection over time (0–3 min and 10–20 min). Somatic α_{2SEP} $GABA_AR$ loss highlighted in red; scale bar, 10 μm. (B) Kymograph showing somatic (left; scale bar, 5 μm) fluorescence intensity over the movie (duration: 60 min) in control (aCSF) conditions and in the presence of low Mg^{2+} and low Mg^{2+}/dAPV (grey bar). Red bar on the right indicates decrease in somatic fluorescence intensity upon low Mg^{2+} treatment and blocking of low Mg^{2+} induced effect by dAPV (B). (C) Time course of somatic α_{2SEP} $GABA_AR$ F/F_0: control (green, n = 7 cells), low Mg^{2+} (blue, n = 8 cells) and low Mg^{2+}/dAPV (dark blue, n = 6 cells). (C') Summary of somatic F/F_0 at 20 min after low Mg^{2+} treatment. Low Mg^{2+} induces a significant decrease ($p < 0.001$) in somatic fluorescence intensity, which is inhibited by application of NMDAR blocker dAPV ($p < 0.001$). ***$p < 0.001$. (For interpretation of the references to colour in this figure legend, the reader is referred to the web version of this article.)

Mg^{2+}/NMDA) caused a loss of α_{2SEP} $GABA_AR$ fluorescence intensity in dendritic clusters (Fig. 4A,B,B') at t = 20 min (control F/F_0: 1.001 ± 0.04, low Mg^{2+}/NMDA F/F_0: 0.799 ± 0.03; $p < 0.01$) suggesting that surface stability of $GABA_AR$s corresponds with the potency of NMDAR activation (Fig. 4C,F). Interestingly, during low Mg^{2+}/NMDA perfusion diffuse (control F/F_0: 1.02 ± 0.03, low Mg^{2+}/NMDA F/F_0: 0.95 ± 0.09, p = 0.58) and total (data not shown) fluorescence intensity in neuronal processes remains unaltered at t = 20 min (Fig. 4D,F). This indicates dispersion of surface $GABA_AR$

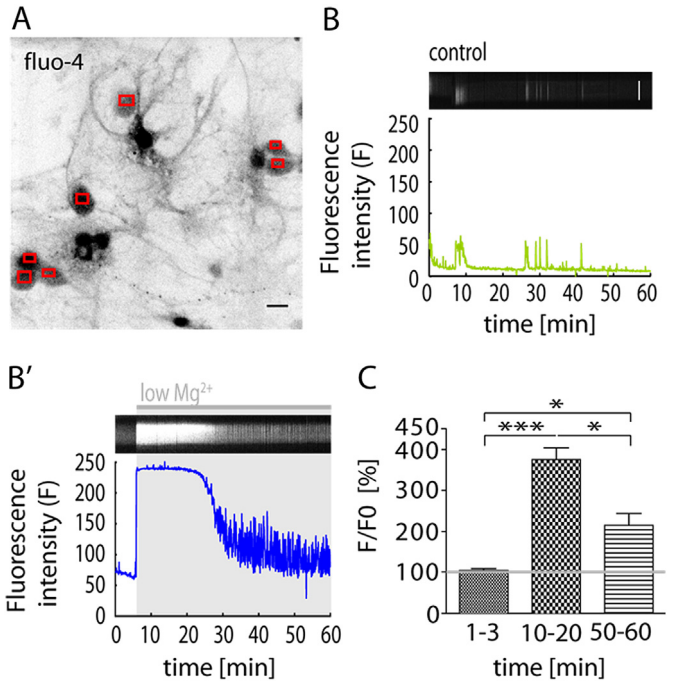

Fig. 3. Low Mg^{2+} treatment induces intracellular Ca^{2+} accumulation. (A) Representative average intensity projection of fluo-4 loaded neurons (coloured squares indicate individual cell bodies). (B) Raw fluorescence intensity of spontaneous Ca^{2+} transients in a neuron (bottom) and correlating kymograph (top; segmented line through somatic ROI) showing fluorescence changes over time under control (aCSF) conditions. (B') Raw fluorescence intensity reporting low Mg^{2+} (grey bar) induced Ca^{2+} accumulation (bottom) and kymograph (top) indicating increase in fluorescence intensity. (C) Quantification of increase in intracellular Ca^{2+} ($n = 21$ cells). Between 10 and 20 min (averaged data points from min 10 to min 20) after low Mg^{2+} induction, intracellular Ca^{2+} is significantly elevated ($p < 0.001$) compared to baseline (averaged data points from min 0 to min 3). At 50–60 min intracellular Ca^{2+} has decreased ($p < 0.001$) compared to 10–20 min and significantly increased ($p = 0.02$) compared to the baseline. $^{*}p < 0.05$, $^{***}p < 0.001$. Scalebar, 10 μm. (For interpretation of the references to colour in this figure legend, the reader is referred to the web version of this article.)

upon low Mg^{2+}/NMDA. Somatic $GABA_AR$ fluorescence intensity is significantly decreased at $t = 10$ min after low Mg^{2+}/NMDA (control F/F_0: 1.00 ± 0.02, low Mg^{2+}/NMDA F/F_0: 0.77 ± 0.059, $p < 0.01$) treatment, however it is not significantly altered at $t = 20$ min (control F/F_0: 0.98 ± 0.03, low Mg^{2+}/NMDA F/F_0: 0.85 ± 0.11, $p = 0.34$) (Fig. 4 E). Although the decrease in somatic surface $GABA_ARs$ fluorescence intensity during low Mg^{2+}/NMDA also occurs rapidly after treatment and is of similar size compared to low Mg^{2+} only treatment, the biphasic recovery phase is shorter in the low Mg^{2+}/NMDA treatment.

3.5. *Calcineurin mediates the decrease of $GABA_A$ receptors from the surface during Low Mg^{2+} induced bursting activity*

We next investigated the signalling mechanisms involved in NMDAR mediated $GABA_AR$ surface decrease during epileptiform bursting activity. Calcineurin is implicated in activity-dependent regulation of GABAergic inhibition and hence could play an important role in Ca^{2+} mediated signalling, we therefore analysed its role in $GABA_AR$ stability during low Mg^{2+} bursting (Lu et al., 2000; Wang et al., 2003; Chen and Wong, 1995; Muir et al., 2010). Cells undergoing epileptiform activity showed a decrease in somatic $GABA_AR$ fluorescence intensity compared to control. We found that treating cells with a calcineurin autoinhibitory peptide did not significantly affect somatic $GABA_AR$ intensity (control F/F_0: 1.07 ± 0.10, control/CAIP F/F_0: 0.95 ± 0.03; $p > 0.05$, one-way ANOVA test and Tukey's multiple comparison post test) showing that calcineurin had no effect at $t = 20$ min in control conditions (Fig. 5C,C'). However, blocking calcineurin activity, inhibited the low Mg^{2+}-induced decrease of surface $GABA_AR$ at the soma at $t = 20$ min significantly (low Mg^{2+} F/F_0: 0.75 ± 0.06, low Mg^{2+}/CAIP F/F_0: 1.043 ± 0.06; $p < 0.05$, one-way ANOVA test and Tukey's multiple comparison post test) (Fig. 5C,C'). These results suggest that calcineurin activation upon Ca^{2+} influx through NMDARs is directly involved in the decrease of surface $GABA_AR$ triggered by epileptiform bursting activity.

4. Discussion

$GABA_ARs$ are a target for a variety of drugs including benzodiazepines, which are of high clinical relevance for first-line treatment of SE. Therefore it is likely that the modulation of surface stability of $GABA_ARs$ induces or supports benzodiazepine pharmacoresistance in patients with SE. To identify potential mechanisms facilitating $GABA_AR$ internalisation, we performed live-imaging on SEP-tagged $GABA_ARs$. The key finding of this study shows epileptiform activity induces activation of calcineurin leading to a decrease in the number of surface $GABA_ARs$ in the soma. This activity-dependent alteration of inhibitory strength is mediated by activation of NMDARs and is parallelled by an increase in intracellular Ca^{2+} which in turn is likely to activate calcineurin. These data identify a signalling mechanism underlying surface $GABA_AR$ decrease during SE and supports studies that report NMDAR activation regulates GABAergic inhibition (Muir et al., 2010; Bannai et al., 2009; Stelzer et al., 1987).

It is known that internalisation of $GABA_ARs$ containing α, γ_2 or $\beta_{2/3}$ subunits is increased during epileptiform activity *in vitro* using low Mg^{2+} or high KCl media (Blair et al., 2004; Goodkin et al., 2008, 2005). Furthermore, it has been demonstrated that $GABA_ARs$ are internalised in chemoconvulsant models of SE *in vivo* (Naylor et al., 2005; Nishimura et al., 2005). Our data supports the hypothesis that $GABA_AR$ internalisation occurs during prolonged seizures, by demonstrating that $GABA_ARs$ which contain the α_2 subunits are decreased during low Mg^{2+} treatment. In the majority of cells this decrease in surface $GABA_ARs$ was biphasic possibly indicating an adaptational switch in inhibitory strength. Interestingly, we observe that this effect occurs preferentially in the soma but less in dendrites. Compartmental internalisation of $GABA_ARs$ during SE has not been reported and the mechanisms underlying this differential regulation are unknown, but there are a number of possibilities. Firstly, it remains to be investigated to what extent intracellular Ca^{2+} buffering systems such as endoplasmic reticulum or mitochondria are contributing to surface stability of $GABA_ARs$ in neurons undergoing epileptiform activity. Expression of signalling proteins in specific subcellular compartments could explain this effect. Secondly, since this study makes use of experiments based on overexpression of $GABA_ARs$, this could account for increased inhibition which could suppress a decrease of $GABA_ARs$ in dendrites specifically. Omitting Mg^{2+} in the extracellular medium of cultured hippocampal neurons triggers a sequence of events leading to neuronal death (Kovac et al., 2012; Yoon et al., 2010). To significantly reduce neuronal cell death, mitochondrial substrate sodium pyruvate was added in our experiments. Although we control for this substitution, it would be interesting to test whether mitochondrial ATP production affects $GABA_AR$ trafficking during prolonged seizures. Thirdly, correlating the amount of intracellular ATP to the trafficking of $GABA_ARs$ could contribute to the understanding of compartmentalised trafficking of $GABA_AR$ during low Mg^{2+} treatment.

A comprehensive body of literature describes that low Mg^{2+} induced epileptiform activity is dependent on increased NMDAR

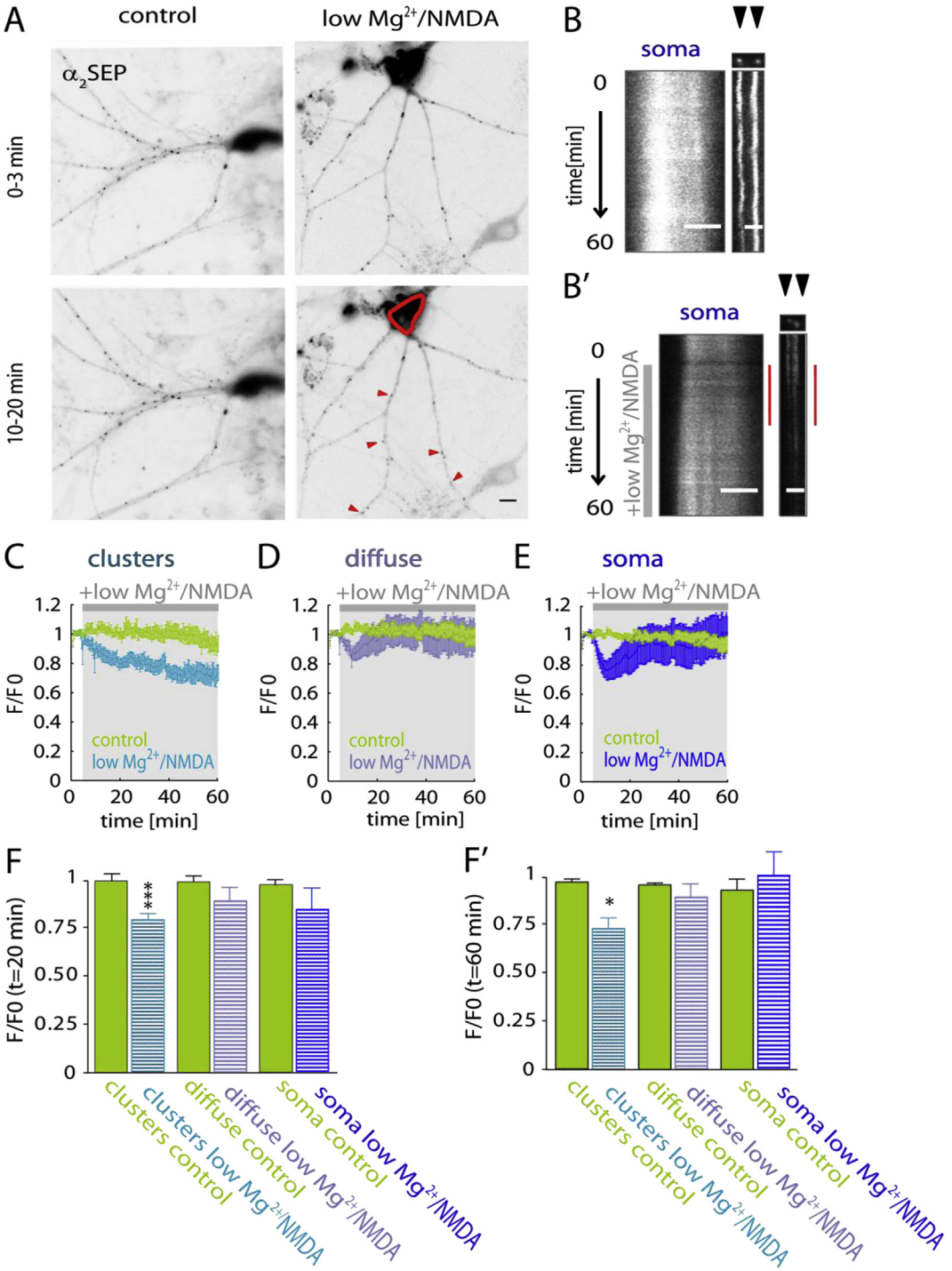

Fig. 4. Clustered α_{2SEP} $GABA_AR$s decrease upon low Mg^{2+}/NMDA treatment. (A) Representative average intensity projection of α_{2SEP} $GABA_AR$ fluorescence in control and low Mg^{2+}/NMDA treated neurons over time (0–3 min and 10–20 min). Somatic α_{2SEP} $GABA_AR$ fluorescence highlighted in red; scale bar, 10 μm. (B) Kymograph showing somatic (left; scale bar, 5 μm) and clustered (right; scale bar, 2 μm) α_{2SEP} $GABA_AR$ fluorescence intensity over the movie in control (aCSF) conditions and in the presence of low Mg^{2+}/NMDA (grey bar). Red bar on the right indicates decrease in somatic α_{2SEP} $GABA_AR$ fluorescence intensity upon low Mg^{2+}/NMDA treatment. (C) Average fluorescence intensity time course of clustered α_{2SEP} $GABA_AR$ F/F_0: control (green, $n = 7$ cells) and low Mg^{2+}/NMDA, (light blue, $n = 9$). (D) Time course of diffuse α_{2SEP} $GABA_AR$ F/F_0: control (green, $n = 7$ cells); low Mg^{2+}, (purple, $n = 9$). (E) Time course of somatic α_{2SEP} $GABA_AR$ F/F_0: control (green, $n = 7$ cells) and low Mg^{2+} (blue, $n = 9$). (F) Bar graph of ROI's F/F_0: clusters (left), diffuse (middle) soma (right). Significant loss of fluorescence in the clusters compared to control at 20 min following after low Mg^{2+} treatment ($p = 0.0008$). Diffuse fluorescence is not altered upon low Mg^{2+} treatment at 20 min ($p = 0.36$) after low Mg^{2+} treatment. Diffuse fluorescence is unaltered following low Mg^{2+} treatment ($t = 20$ min; $p = 0.58$) compared to control. (F') At 60 after low Mg^{2+} treatment clustered fluorescence intensity is still significantly reduced ($p < 0.001$), diffuse ($p = 0.99$) and somatic ($p = 0.63$) fluorescence are not significantly altered. $^*p < 0.05$, $^{***}p < 0.001$. (For interpretation of the references to colour in this figure legend, the reader is referred to the web version of this article.)

activity (Coan and Collingridge, 1985, 1987; Tancredi et al., 1990; Albowitz et al., 1997; Westerhoff et al., 1995; Gulyás-Kovács et al., 2002; Mangan and Kapur, 2004), therefore we tested whether the somatic surface $GABA_AR$ decrease was mediated by NMDAR activity. Our experiments confirm this hypothesis by reporting that the decrease in surface $GABA_AR$ was blocked by application of NMDAR blocker dAPV. To our knowledge this is the first study showing a direct regulation of $GABA_ARs$ by NMDAR activation

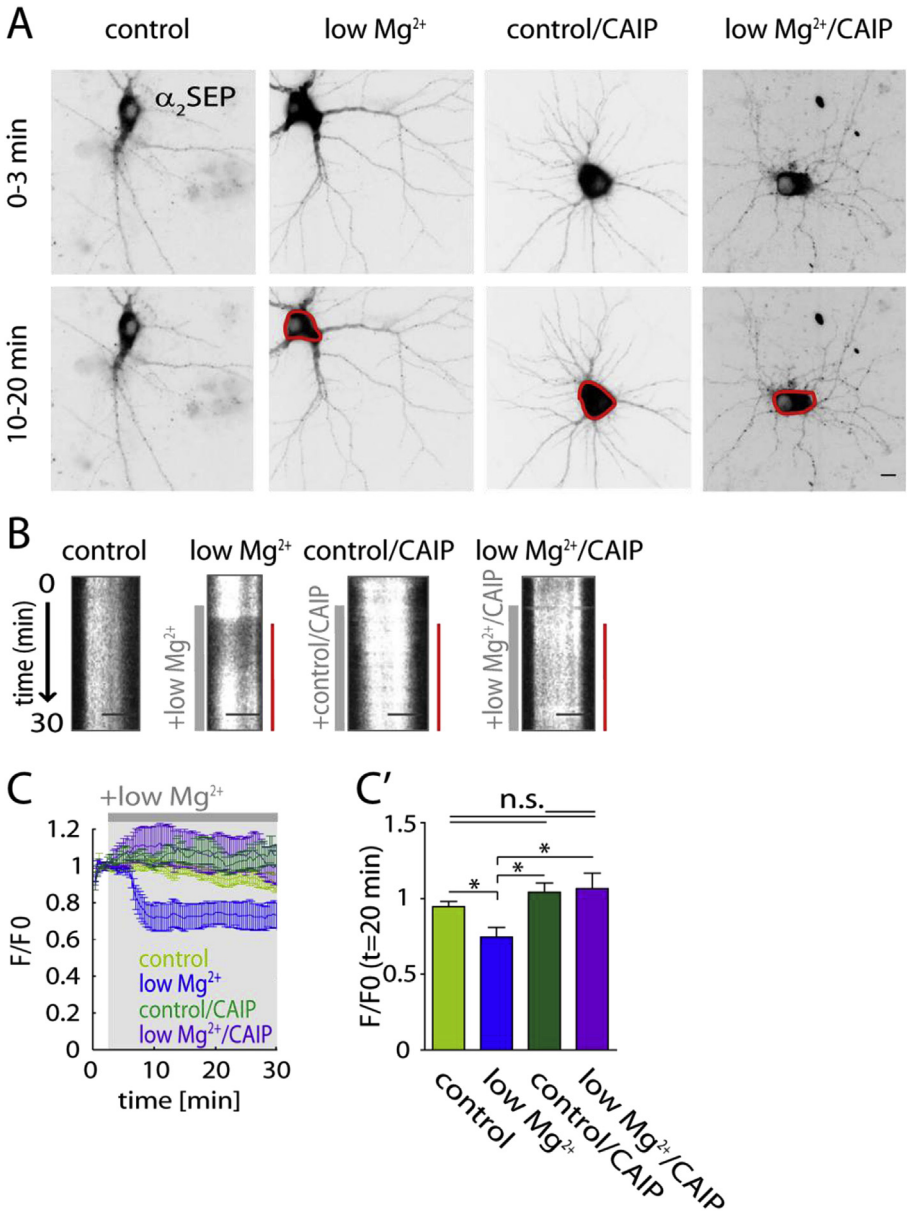

Fig. 5. Calcineurin mediates the decrease of somatic surface $GABA_AR$s during low Mg^{2+} treatment. (A) Representative images of α_{2SEP} $GABA_AR$ fluorescence in control, control with CAIP (control/CAIP), low Mg^{2+} and low Mg^{2+} with CAIP (low Mg^{2+}/CAIP) treated neurons as an average intensity projection over time (0–3 min and 10–20 min). Scale bar, 10 μm. (B) Kymographs showing somatic (scale bar: 5 μm) fluorescence intensity over the movie (duration: 30 min) in control conditions, control/CAIP and in the presence of low Mg^{2+} and low Mg^{2+}/CAIP (grey bar). Red bar on the right indicates decrease in somatic fluorescence intensity upon low Mg^{2+} treatment. (C) Average fluorescence intensity of α_{2SEP} $GABA_AR$ F/F0: control (light green, $n = 6$ cells); low Mg^{2+} (dark blue, $n = 7$ cells); control/CAIP (dark green, $n = 6$); low Mg^{2+}/CAIP (purple, $n = 6$). (C') Bar graph showing quantification of α_{2SEP} $GABA_AR$ F/F_0 at $t = 20$ min. Somatic fluorescence intensity of low Mg^{2+} treated cells is significantly decreased compared to control at $t = 20$ min (dark blue bar, $p < 0.05$). Treatment of low Mg^{2+} perfused cells with a calcineurin autoinhibitory peptide prevents the change in fluorescence intensity (dark green bar, $p < 0.05$). Treatment with calcineurin autoinhibitory peptide alone does not significantly alter the fluorescence intensity of $GABA_AR$ α_{2SEP} (magenta bar, $p > 0.05$). *$p < 0.05$. (For interpretation of the references to colour in this figure legend, the reader is referred to the web version of this article.)

during low Mg^{2+} induced epileptiform activity. However, whether the same process underlies the regulation of $GABA_AR$s during epileptiform activity induced by different approaches (Goodkin et al., 2008; Laurén et al., 2005) remains to be determined. The observation that NMDAR activation and rises in internal calcium are common to all models of SE (Raza et al., 2004; Rice and DeLorenzo, 1998; Mazarati and Wasterlain, 1999) would suggest that this is a universal mechanism.

Interestingly, the direct activation of NMDARs with low Mg^{2+} and NMDA induces a potent change in surface stability of $GABA_AR$ clusters. The mechanisms underlying this modulation need further investigation, however dephosphorylation of $GABA_AR$ γ2 subunits could play a role (Muir et al., 2010). Our data suggest that potency of NMDAR activation correlates with the extent of $GABA_AR$ modification, and may explain the synergistic effect of benzodiazepines and NMDAR antagonists in the treatment of SE (Rice and DeLorenzo, 1999; Martin and Kapur, 2008).

Ca^{2+} influx from the extracellular environment through NMDARs can alter the stability of inhibitory neurotransmitter receptors (Bannai et al., 2009; Muir et al., 2010). Bannai et al. showed that diffusion dynamics of $GABA_AR$s too are tuned by Ca^{2+} entry from the extracellular space. Indeed, here we report an increase in

intracellular Ca^{2+} concentration during low Mg^{2+} treatment. Moreover, Ca^{2+} levels correlate with the temporal dynamics of the low Mg^{2+} induced effect on $GABA_A$Rs. This indicates that fast Ca^{2+}-signalling could indirectly be altering $GABA_A$Rs surface stability. Although technically challenging, it would be of major interest to simultaneously dual record Ca^{2+} dynamics and $GABA_A$Rs surface stability to better address the relationship of low Mg^{2+} induced spiking activity and $GABA_A$R trafficking on a single cell level.

Surface stability of $GABA_A$Rs is regulated by multiple processes which are facilitated by direct or indirect interaction with trafficking proteins (Marsden et al., 2007; Jacob et al., 2008). Our experiments further emphasise the relationship of indirect signalling via intracellular Ca^{2+} sensing proteins to stabilise neurotransmitter receptors. Downstream effects of Ca^{2+} sensing proteins such as calmodulin orchestrate a number of target proteins and can trigger selective effects on surface $GABA_A$R stability. It is known that increased phosphorylation of $GABA_A$Rs contributes to surface stability (Saliba et al., 2012). Terunuma et al. demonstrated deficits in $GABA_A$R phosphorylation during SE mediated by protein kinase C (Terunuma et al., 2008). Opposingly, dephosphorylation induces declustering and increases the diffusion dynamics of $GABA_A$Rs (Muir et al., 2010). Calcineurin has been shown to interact with $GABA_A$Rs via the γ_2 subunit and it modulates neuronal inhibition. Interestingly, basal and maximal activity of calcineurin is increased (Kurz et al., 2001) and subcellular distribution is altered (Kurz et al., 2003) in SE *in vivo*. However, it has been poorly investigated whether calcineurin mediates the decrease in surface $GABA_A$Rs (Wang et al., 2009). We identify calcineurin as a mediator of the decrease in surface $GABA_A$R and therefore, provide a mechanism of inhibitory modulation during SE, and a potential target for therapy. Moreover, this study is the first to demonstrate a decrease in surface $GABA_A$Rs by live-imaging in hippocampal neurons during SE. The identification of the underlying trafficking mechanism could account for resistance to benzodiazepines and could have additive effects on duration or frequency of seizure activity. Further research is needed to develop more effective therapeutic strategies against SE to which this study will contribute.

Acknowledgements

This work was supported by grants from the UK Medical Research Council, the Wellcome Trust to J.T.K. and UCL School of Life and Medical Sciences Grand Challenge Studentships.

Appendix A. Supplementary data

Supplementary data related to this article can be found at http://dx.doi.org/10.1016/j.neuropharm.2014.09.014.

References

Albowitz, B., König, P., Kuhnt, U., 1997. Spatiotemporal distribution of intracellular calcium transients during epileptiform activity in guinea pig hippocampal slices. J. Neurophysiol. 77 (1), 491–501.

Bannai, H., et al., 2009. Activity-dependent tuning of inhibitory neurotransmission based on GABAAR diffusion dynamics. Neuron 62 (5), 670–682.

Blair, R.E., et al., 2004. Epileptogenesis causes acute and chronic increases in GABAA receptor endocytosis that contributes to the induction and maintenance of seizures in the hippocampal culture model of acquired epilepsy. J. Pharmacol. Exp. Ther. 310 (3), 871–880. Available at: http://www.ncbi.nlm.nih.gov/pubmed/15084648 (accessed 11.06.14.).

Bogdanov, Y., et al., 2006. Synaptic GABAA receptors are directly recruited from their extrasynaptic counterparts. EMBO J. 25 (18), 4381–4389. Available at: http://www.pubmedcentral.nih.gov/articlerender.fcgi?artid=1570424&tool=pmcentrez&rendertype=abstract (accessed 28.05.14.).

Brünig, I., et al., 2002. Intact sorting, targeting, and clustering of gamma-aminobutyric acid A receptor subtypes in hippocampal neurons in vitro. J. Comp. Neurol. 443 (1), 43–55.

Chen, Q.X., Wong, R.K., 1995. Suppression of GABAA receptor responses by NMDA application in hippocampal neurones acutely isolated from the adult guinea-pig. J. Physiol. 482 (Pt 2), 353–362.

Coan, E.J., Collingridge, G.L., 1987. Characterization of an N-methyl-d-aspartate receptor component of synaptic transmission in rat hippocampal slices. Neuroscience 22 (1), 1–8. Available at: http://www.sciencedirect.com/science/article/pii/0306452287901928 (accessed 15.06.14.).

Coan, E.J., Collingridge, G.L., 1985. Magnesium ions block an N-methyl-d-aspartate receptor-mediated component of synaptic transmission in rat hippocampus. Neurosci. Lett. 53 (1), 21–26. Available at: http://www.sciencedirect.com/science/article/pii/0304394085900916 (accessed 15.06.14.).

DeLorenzo, R.J., Pal, S., Sombati, S., 1998. Prolonged activation of the N-methyl-D-aspartate receptor-Ca^{2+} transduction pathway causes spontaneous recurrent epileptiform discharges in hippocampal neurons in culture. Proc. Natl. Acad. Sci. U. S. A. 95 (24), 14482–14487.

Dodrill, C.B., Wilensky, A.J., 1990. Intellectual impairment as an outcome of status epilepticus. Neurology 40 (5 Suppl. 2), 23–27. Available at: http://www.ncbi.nlm.nih.gov/pubmed/2185437 (accessed 11.06.14.).

Goodkin, H.P., et al., 2008. Subunit-specific trafficking of GABA(A) receptors during status epilepticus. J. Neurosci. 28 (10), 2527–2538. Available at: http://www.pubmedcentral.nih.gov/articlerender.fcgi?artid=2880323&tool=pmcentrez&rendertype=abstract.

Goodkin, H.P., Yeh, J.-L., Kapur, J., 2005. Status epilepticus increases the intracellular accumulation of GABAA receptors. J. Neurosci. 25 (23), 5511–5520. Available at: http://www.pubmedcentral.nih.gov/articlerender.fcgi?artid=2878479&tool=pmcentrez&rendertype=abstract.

Gulyás-Kovács, A., et al., 2002. Comparison of spontaneous and evoked epileptiform activity in three in vitro epilepsy models. Brain Res. 945 (2), 174–180. Available at: http://www.sciencedirect.com/science/article/pii/S0006899302027518 (accessed 15.06.14.).

Jacob, T.C., Moss, S.J., Jurd, R., 2008. Reviews GABA A receptor trafficking and its role in the dynamic modulation of neuronal inhibition. Nature 9 (May), 331–343. Available at: http://www.ncbi.nlm.nih.gov/pmc/articles/PMC2709246/.

Kittler, J.T., et al., 2000. Constitutive endocytosis of GABAA receptors by an association with the adaptin AP2 complex modulates inhibitory synaptic currents in hippocampal neurons. J. Neurosci. 20 (21), 7972–7977. Available at: http://www.jneurosci.org/content/20/21/7972.short (accessed 11.06.14.).

Kittler, J.T., et al., 2004. Huntingtin-associated protein 1 regulates inhibitory synaptic transmission by modulating γ-aminobutyric acid type A receptor membrane trafficking. Proc. Natl. Acad. Sci. U. S. A. 101 (34), 12736–12741. Available at: http://discovery.ucl.ac.uk/9648/.

Kovac, S., et al., 2012. Prolonged seizure activity impairs mitochondrial bioenergetics and induces cell death. J. Cell Sci. 125 (Pt 7), 1796–1806. Available at: http://jcs.biologists.org/content/125/7/1796.long (accessed 28.03.14.).

Kurz, J.E., et al., 2001. A significant increase in both basal and maximal calcineurin activity in the rat pilocarpine model of status epilepticus. J. Neurochem. 78 (2), 304–315. Available at: http://doi.wiley.com/10.1046/j.1471-4159.2001.00426.x (accessed 19.06.14.).

Kurz, J.E., et al., 2003. Status epilepticus-induced changes in the subcellular distribution and activity of calcineurin in rat forebrain. Neurobiol. Dis. 14 (3), 483–493.

Laurén, H.B., et al., 2005. Kainic acid-induced status epilepticus alters GABA receptor subunit mRNA and protein expression in the developing rat hippocampus. J. Neurochem. 94 (5), 1384–1394. Available at: http://www.ncbi.nlm.nih.gov/pubmed/15992369 (accessed 13.07.14.).

Lothman, E.W., 1990. The biochemical basis and pathophysiology of status epilepticus. Neurology 40, 13–23.

Lu, Y.M., et al., 2000. Calcineurin-mediated LTD of GABAergic inhibition underlies the increased excitability of CA1 neurons associated with LTP. Neuron 26 (1), 197–205. Available at: http://www.sciencedirect.com/science/article/pii/S0896627300811502 (accessed 15.06.14.).

Luscher, B., Fuchs, T., Kilpatrick, C.L., 2011. GABAA receptor trafficking-mediated plasticity of inhibitory synapses. Neuron 70 (3), 385–409. Available at: http://www.pubmedcentral.nih.gov/articlerender.fcgi?artid=3093971&tool=pmcentrez&rendertype=abstract (accessed 24.05.14.).

Mangan, P.S., Kapur, J., 2004. Factors underlying bursting behavior in a network of cultured hippocampal neurons exposed to zero magnesium. J. Neurophysiol. 91 (2), 946–957. Available at: http://www.pubmedcentral.nih.gov/articlerender.fcgi?artid=2892720&tool=pmcentrez&rendertype=abstract.

Marsden, K.C., et al., 2007. NMDA receptor activation potentiates inhibitory transmission through GABA receptor-associated protein-dependent exocytosis of GABA(A) receptors. J. Neurosci. Off. J. Soc. Neurosci. 27 (52), 14326–14337. Available at: http://www.ncbi.nlm.nih.gov/pubmed/18160640 (accessed 05.06.14.).

Martin, B.S., Kapur, J., 2008. A combination of ketamine and diazepam synergistically controls refractory status epilepticus induced by cholinergic stimulation. Epilepsia 49 (2), 248–255. Available at: http://www.pubmedcentral.nih.gov/articlerender.fcgi?artid=2844443&tool=pmcentrez&rendertype=abstract (accessed 13.07.14.).

Mazarati, A.M., Wasterlain, C.G., 1999. N-methyl-d-asparate receptor antagonists abolish the maintenance phase of self-sustaining status epilepticus in rat. Neurosci. Lett. 265 (3), 187–190. Available at: http://www.sciencedirect.com/science/article/pii/S0304394099002384 (accessed 13.07.14.).

Muir, J., et al., 2010. NMDA receptors regulate GABAA receptor lateral mobility and clustering at inhibitory synapses through serine 327 on the γ2 subunit. Proc.

Natl. Acad. Sci. U. S. A. 107 (38), 16679–16684. Available at: http://discovery.ucl.ac.uk/168536/.
Mukherjee, J., et al., 2011. The residence time of GABAARs at inhibitory synapses is determined by direct binding of the receptor 1 subunit to gephyrin. J. Neurosci. 31 (41), 14677–14687.
Naylor, D.E., Liu, H., Wasterlain, C.G., 2005. Trafficking of GABA(A) receptors, loss of inhibition, and a mechanism for pharmacoresistance in status epilepticus. J. Neurosci. 25 (34), 7724–7733. Available at: http://www.ncbi.nlm.nih.gov/pubmed/16120773.
Nishimura, T., et al., 2005. Altered expression of GABA(A) and GABA(B) receptor subunit mRNAs in the hippocampus after kindling and electrically induced status epilepticus. Neuroscience 134 (2), 691–704. Available at: http://www.ncbi.nlm.nih.gov/pubmed/15951123.
Panzanelli, P., et al., 2011. Distinct mechanisms regulate GABAA receptor and gephyrin clustering at perisomatic and axo-axonic synapses on CA1 pyramidal cells. J. Physiol. 589 (20), 4959–4980. Available at: http://www.pubmedcentral.nih.gov/articlerender.fcgi?artid=3224886&tool=pmcentrez&rendertype=abstract.
Petrini, E.M., et al., 2014. Synaptic recruitment of gephyrin regulates surface GABAA receptor dynamics for the expression of inhibitory LTP. Nat. Commun. 5, 3921. Available at: http://www.ncbi.nlm.nih.gov/pubmed/24894704.
Pritchett, D.B., et al., 1989. Importance of a novel GABAA receptor subunit for benzodiazepine pharmacology. Nature 338 (6216), 582–585. Available at: http://dx.doi.org/10.1038/338582a0 (accessed 30.05.14.).
Raza, M., et al., 2004. Evidence that injury-induced changes in hippocampal neuronal calcium dynamics during epileptogenesis cause acquired epilepsy. Proc. Natl. Acad. Sci. U. S. A. 101 (50), 17522–17527. Available at: http://www.pubmedcentral.nih.gov/articlerender.fcgi?artid=535000&tool=pmcentrez&rendertype=abstract (accessed 13.07.14.).
Rice, A.C., DeLorenzo, R.J., 1998. NMDA receptor activation during status epilepticus is required for the development of epilepsy. Brain Res. 782 (1–2), 240–247. Available at: http://www.ncbi.nlm.nih.gov/pubmed/9519269 (accessed 13.07.14.).
Rice, A.C., DeLorenzo, R.J., 1999. N-methyl-D-aspartate receptor activation regulates refractoriness of status epilepticus to diazepam. Neuroscience 93 (1), 117–123. Available at: http://www.ncbi.nlm.nih.gov/pubmed/10430476 (accessed 13.07.14.).
Robinson, H.P., et al., 1993. Periodic synchronized bursting and intracellular calcium transients elicited by low magnesium in cultured cortical neurons. J. Neurophysiol. 70 (4), 1606–1616. Available at: http://jn.physiology.org/content/70/4/1606.abstract (accessed 14.05.14.).
Saliba, R.S., Kretschmannova, K., Moss, S.J., 2012. Activity-dependent phosphorylation of GABAA receptors regulates receptor insertion and tonic current. EMBO J. 31 (13), 2937–2951. Available at: http://www.ncbi.nlm.nih.gov/pubmed/22531784.
Sombati, S., Delorenzo, R.J., 1995. Recurrent spontaneous seizure activity in hippocampal neuronal networks in culture. J. Neurophysiol. 73 (4), 1706–1711.
Stelzer, A., Slater, N.T., ten Bruggencate, G., 1987. Activation of NMDA receptors blocks GABAergic inhibition in an in vitro model of epilepsy. Nature 326 (6114), 698–701. Available at: http://dx.doi.org/10.1038/326698a0 (accessed 05.07.14.).
Sutter, R., et al., 2013. Mortality and recovery from refractory status epilepticus in the intensive care unit: a 7-year observational study. Epilepsia 54 (3), 502–511. Available at: http://www.ncbi.nlm.nih.gov/pubmed/23294049 (accessed 28.05.14.).
Tancredi, V., et al., 1990. Low magnesium epileptogenesis in the rat hippocampal slice: electrophysiological and pharmacological features. Brain Res. 511 (2), 280–290.
Terada, H., et al., 2003. Inhibition of excitatory neuronal cell death by cell-permeable calcineurin autoinhibitory peptide. J. Neurochem. 87 (5), 1145–1151.
Terunuma, M., et al., 2008. Deficits in phosphorylation of GABA(A) receptors by intimately associated protein kinase C activity underlie compromised synaptic inhibition during status epilepticus. J. Neurosci. 28 (2), 376–384. Available at: http://discovery.ucl.ac.uk/134982/.
Thévenaz, P., Ruttimann, U.E., Unser, M., 1998. A pyramid approach to subpixel registration based on intensity. IEEE Trans. Image Process. 7 (1), 27–41.
Tretter, V., et al., 2008. The clustering of GABA(A) receptor subtypes at inhibitory synapses is facilitated via the direct binding of receptor alpha 2 subunits to gephyrin. J. Neurosci. 28 (6), 1356–1365. Available at: http://www.ncbi.nlm.nih.gov/pubmed/18256255.
Trinka, E., Höfler, J., Zerbs, A., 2012. Causes of status epilepticus. Epilepsia 53 (Suppl. 4), 127–138.
Wang, A., et al., 2009. Calcineurin-mediated GABAA receptor dephosphorylation in rats after kainic acid-induced status epilepticus. Seizure 18 (7), 519–523.
Wang, J., et al., 2003. Interaction of calcineurin and type-A GABA receptor gamma 2 subunits produces long-term depression at CA1 inhibitory synapses. J. Neurosci. Off. J. Soc. Neurosci. 23 (3), 826–836. Available at: http://www.ncbi.nlm.nih.gov/pubmed/12574411 (accessed 27.03.14.).
Westerhoff, C.H., Domann, R., Witte, O.W., 1995. Inhibitory mechanisms in epileptiform activity induced by low magnesium. Pflugers Arch. 430 (2), 238–245.
Yoon, J.J., et al., 2010. Effect of low Mg^{2+} and bicuculline on cell survival in hippocampal slice cultures. Int. J. Neurosci. 120 (12), 752–759. Available at: http://www.ncbi.nlm.nih.gov/pubmed/20942591.